Measurement of Magnetic Field Using Collaborative AUVs

Jesse Pentzer, Brendan Crosbie, Thomas Bean, John Canning, James Frenzel, Michael Anderson, Dean Edwards
Center for Intelligent Systems Research, University of Idaho, Moscow, ID 83844-1024

***Abstract*-This paper describes an effort to adapt a fleet of autonomous underwater vehicles (AUVs) for the measurement of the magnetic signature of surface ships. Currently, two such vehicles have been upgraded with the necessary navigation and measurement hardware to perform magnetic measurements. Initial testing has been performed at the Naval Acoustic Research Detachment at Lake Pend Oreille, Idaho. Two vehicles have leveraged formation control algorithms originally developed for mine countermeasure missions to operate collaboratively. In the testing area, changes in ambient field were measured to be ~1,000-2,000 nT. Over one square meter area segments, the standard deviation of total field measurements was below 25 nT. When a steel barge was located in the testing area, localized fields of ~50,000 nT to ~62,000 nT were observed.**

I. Introduction

An important application of autonomous underwater vehicles (AUVs) is to perform measurements in an underwater environment. Historically, the majority of measurements have been performed with an individual AUV. In this paper, experiments are described in which multiple, collaborating AUVs are used to spatially sample the ambient magnetic field. Collaboration between AUVs ensures adequate measurement coverage, even in the presence of vehicle malfunction, and allows for correlation between magnetic data and accurate AUV position estimates. The eventual application is the measurement of the magnetic signature of a moving surface vessel with multiple AUVs operating cooperatively.

Single AUVs have been utilized extensively as autonomous sensor platforms. In 2006, tests using multiple types of AUVs to individually sample bathymetric data and water mass properties were described [1]. Results of utilizing single AUVs with side scan sonar for mine-like-object detection were also included. Also in 2006, the use of an AUV to map coral mounds while recording current, salinity, and temperature data was reported [2]. In 2007, an AUV was equipped to measure water properties near underwater methane vents [3].

Less work has been done on performing measurements with multiple AUVs. In 2003, three autonomous underwater gliders were used to measure ocean temperature, but there was no communication between individual gliders [4]. In 2004, research was presented of AUVs being used to detect mine-like-objects under the control of a human operator. It was mentioned that the AUVs were capable of completely autonomous operation and inter-vehicle communication, but no such experiments were described [5]. In [6], research into the control of a heterogeneous fleet of vehicles using a moving baseline technique was presented. The eventual application would be mine-countermeasure missions. Similar research also involving a heterogeneous fleet of vehicles and moving baseline navigation was presented in [7]. In 2003-2005, three glider AUVs, six repeater nodes, and two gateway buoys were reported to function together [8]. A network of sensor nodes communicating with an AUV was presented in 2005 [9].

More recently, Dunbabin et al. presented a multi-robot system capable of cooperative navigation, whereby robots can join together to traverse long distances [10]. Experimental results in a controlled environment were discussed in which the AUV used communication to interact cooperatively with an underwater sensor network. In [11], Haraksim et al. outline two leader-follower scenarios and the associated communication requirements. This work was then validated in a set of sea trials in support of the GREX project [12]. Cooperative navigation allowed two vehicles with different speed capabilities to navigate a course in a coordinated manner through the exchange of acoustic messages.

Very little research has been published on the measurement of a magnetic field using an AUV or multiple AUVs. In 2007, experiments were reported involving a single AUV measuring the magnetic signature of a surface vessel [13]. The authors of the paper concluded that the shortcomings of the test were inaccuracies in the positioning of the AUV, the time required to complete a measurement using one AUV, and the lack of knowledge of the target ship attitude.

The first shortcoming of AUV position inaccuracy can be addressed by improving both real-time and post-processing navigation algorithms. Such research was presented in [14], where the position estimation of the vehicles was shown to be accurate to within 0.74 m in the horizontal plane. Utilizing multiple AUVs decreases the time required for signature measurement, another shortcoming in previous research.

This paper will present preliminary measurements of an ambient magnetic field by two AUVs operating cooperatively. Section II will outline the vehicle and important subsystems while Section III will detail the formation control and communications needed for the AUVs to operate cooperatively. The area in which the experiments were performed will be described in Section IV, and the results of the experiments will be presented in Section V. Finally, the conclusions and suggestions for future work will be discussed in Section VI.

II. Description of Vehicles

The vehicles utilized to perform the fleet operations and take measurements were miniature AUVs based on the design of Dan Stillwell et al., Virginia Tech [15]. The AUVs were approximately 0.737 m long and 10.16 cm in diameter. A picture of one of the AUVs is shown in Fig. 1.

978-1-4244-5222-4/10/$26.00 ©2010 IEEE

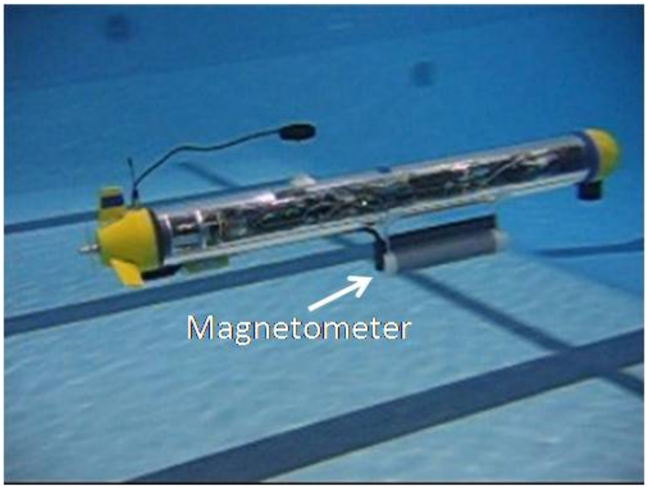

Figure 1. Photograph of test vehicle during initial pool testing.

The original AUV design consisted of an acrylic hull and aluminum frame. Also, the nose cone and tail cone were made of PVC, resulting in a small vehicle signature. Magnetically permeable components such as screws were replaced with non-permeable analogs to further reduce the induced field of the vehicle. Circuit boards were degaussed to remove permanent magnetization of metal components such as Ethernet connectors and memory card receptors.

The vehicles were equipped with tri-axial fluxgate type magnetometers capable of measuring over a range of ±100,000 nT on each channel. The output range of the sensor was ±10 V. Each magnetometer channel was sampled at 16,700 Hz with 16-bit resolution and stored on a flash memory card. The magnetometer was mounted below the vehicle and towards the front to minimize noise in the measurements from the motor.

Each AUV utilized an acoustic Micro-modem system designed and fabricated by the Woods Hole Oceanographic Institute [16]. The acoustic modem enabled multiple AUVs to communicate through 13-bit and 32-byte messages. These messages were utilized to share information necessary for formation control, described in section III. More detailed descriptions of other AUV components are given in [14] and [17].

The acoustic modem also allowed vehicles to obtain ranges from bottom mounted transponders to be used in navigation algorithms. An extended Kalman Filter (EKF) was used on the AUV to estimate the position, heading, and forward speed of the vehicle by combining information from ranges, an inertial measurement unit (IMU), and a magnetic compass [14, 18]. The IMU measured acceleration and angular rotation rate about three orthogonal axes. The prediction rate of the filter was 4 Hz, and measurements of heading and forward speed were available to update the EKF at each time step. Measurements of heading came from a magnetic compass while measurements of forward speed came from a linear correlation relating motor RPM to forward speed. The acoustic ranges were available once every fifteen seconds.

A larger EKF was used in post-processing that utilized all outputs of the IMU to achieve an improved estimate of vehicle position and attitude [14]. The larger EKF could not be run on the vehicle due to computational limitations of the current processor. Since [14] was published, a Rauch-Tung-Striebel (RTS) smoothing algorithm [19, 20] was implemented to improve the estimate of the state. The RTS smoothing algorithm is a two pass method that utilizes all past and future information available to the filter to create an optimum estimate of a state. To operate the algorithm, the state vectors before and after the EKF update, X_k^- and X_k^+, and the state covariance arrays at the same times, P_k^- and P_k^+, must be stored at each time step. Also, the state transition matrix, F_k, must also be stored at each time step during a normal, forward EKF run. The smoother is initialized with the last state stored at $k=N$ using

$$X_{[s]N} = X_N^+, \tag{1}$$

where $X_{[s]N}$ is the smoothed estimate at the final time step N.

The algorithm operates by moving backwards in time through the stored data from the forward run of the EKF. At each time step the intermediate calculation

$$A_k = P_k^+ F_k^T (P_{k+1}^-)^{-1} \tag{2}$$

is performed, followed by the calculation of the smoothed estimate, $X_{[s]k}$, at the current time step,

$$X_{[s]k} = X_k^+ + A_k\left(X_{[s]k+1} - X_{k+1}^-\right). \tag{3}$$

III. Multi-Vehicle Formation Control

The AUVs were deployed as a formation and used a behavior-based control system to perform cooperative operations. One vehicle was assigned to be a leader, though each vehicle was capable of the leader function and could be dynamically re-assigned to this task. Additionally, the leader function was not associated with a specific formation position. The leader set the pace for the formation and maintained the formation integrity by employing formation maintenance algorithms.

All cooperative behaviors were performed while the vehicles maintained a geometric formation. Formation-flying was implemented using a leader-follower regulation algorithm [21-24] in each vehicle. The algorithm contained two components: path following and formation control. The basics of the control algorithms for three vehicles in formation are diagrammed in Fig. 2.

Each vehicle was assigned a unique position in terms of path and formation offsets, δ and Δ, with respect to the primary formation position. For the formation shown in Fig. 2a, the primary formation position was swimmer 1. For simplicity, the leader is depicted as occupying this primary position. However, the leader may be in any position of the formation. The control law for an individual vehicle was

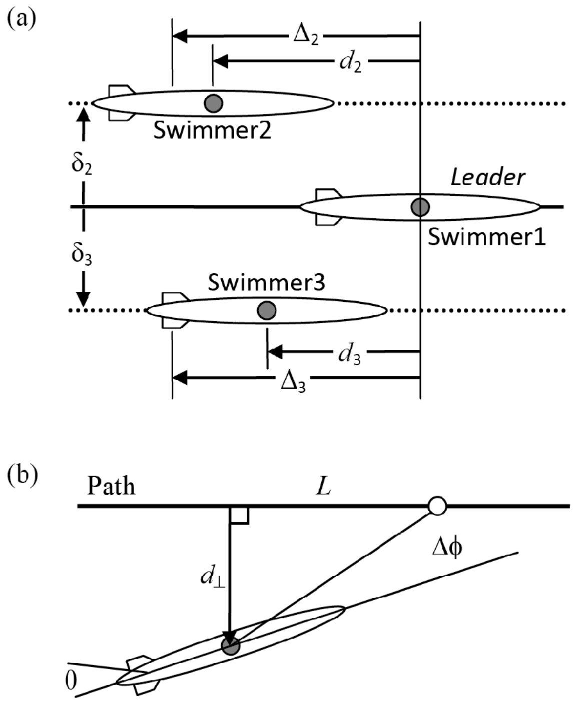

Figure 2. Formation geometry (a) and path following (b).

$$u = \underbrace{k_v\left(v - v_{ref}\right)}_{Path\ Following} + \underbrace{k_d(d - \Delta)}_{Formation\ Control}, \qquad (4)$$

$$\theta = \underbrace{k_{\Delta\phi}\Delta\phi + k_{\int d}\int d_{\perp}dt}_{Path\ Following}. \qquad (5)$$

Equation (4) calculated the commanded velocity, u, in terms of the measured speed, v, the reference velocity, v_{ref}, and the distance from the primary formation position, d. The value Δ was the desired formation offset from the primary formation position. Equation (5) controlled the heading control surface angle, θ, by calculating the difference between the actual and desired heading, $\Delta\phi$, then adding a trim control based on the perpendicular distance to the path, $d_\perp$. The trim control was an integrator control that added up to 5^o of trim to the rudder settings. The other values: k_v, k_d, $k_{\Delta\phi}$ and $k_{\int d}$, were the controller gains.

The formation flying algorithm is similar to others that have been applied to multiple autonomous vehicles, and has known properties of stability. The control laws (4) and (5) require that each vehicle sense inertial position and the relative distance to the primary formation position. This topology has been shown to be locally stable for continuous and discrete cases [25], and similar algorithms under certain conditions have been shown to be globally stable in the presence of delay, decentralized communication links, and missing communications [26, 27].

Formation flying was enabled by using a Time-Division-Multiple-Access (TDMA) communications approach. In this approach, each vehicle was given the opportunity to broadcast a 13-bit message in sequence during each communications cycle. This message was broadcast in parallel to all other vehicles and supplied information about the formation position and status of the transmitting vehicle. The 13-bit message also included information on which other vehicles the transmitting vehicle had heard from in the previous communication cycle. The results presented in this paper came from experiments with a two vehicle formation, so a 15 second communication cycle was used.

Once in every communication cycle, the leader sent a 32-byte message to all other vehicles. The estimated progress of the formation along the waypoint path from the perspective of the leader vehicle was included in this message. Each vehicle that received the 32-byte message compared the formation progress with its own progress to calculate a relative distance to the primary formation position, d, which is used in control law (4).

A single set of waypoints were stored in each vehicle along with formation offset values, δ and Δ, for all possible formation positions. Once a formation position was established for a vehicle, the values of δ and Δ were used with (4) and (5) to control the vehicle along the proper course.

The leader vehicle dynamically maintained the integrity of the formation by using Formation Maintenance algorithms as described in [21]. While underway, the leader constantly monitored the communications of the other vehicles. When the leader determined that a position in the formation was not properly filled, the leader sent a vehicle replacement command in the 32-byte message. The vehicle replacement message reassigned a vehicle occupying a lesser formation position to the empty position. The reassigned vehicle subsequently reported his position using a 13-bit message and changed to the appropriate formation offset values, δ and Δ, for the new position. With a fleet of two vehicles, as described in this paper, the vehicles were instructed to stay in the swimmer 1 and swimmer 2 positions.

IV. Description of Testing Area

Testing of the AUV fleet was conducted at the southern end of Lake Pend Oreille, ID at the Naval Acoustic Research Detachment (ARD). The AUVs were operated in an ARD secured area with a nominal water depth of 15 m. A topside tracking array developed jointly by ARD and the University of Idaho (UI) has been installed in the area.

The topside tracking system provides an independent measure of the position of the AUV in all three dimensions. At the same time, it functions as the navigation transponders for the AUVs. Tests on the tracking system have shown it to be accurate to within 10 cm when tracking the AUVs. The tracking data has been used extensively in improving the navigation algorithms operating on the vehicles and used in post processing.

V. Results

The results from initial in-water testing will be presented in two steps. First, an analysis of the formation flying of the vehicles will be presented in Section V.A. The multi-vehicle position data presented was collected with the AUVs operating on the surface and is the output of the post-processing EKF with smoothing. In Section V.B, magnetic measurements taken during multi-vehicle runs and measurements recorded by a single AUV traveling under a steel barge will be discussed.

A. Formation Control Results

Two UI AUVs have been equipped with the necessary equipment to measure magnetic fields, allowing a formation of two vehicles to test formation control algorithms. Fig. 3 shows the vehicle tracks from a formation mission. The red line shows the path taken by vehicle 1, and the blue line shows the path taken by vehicle 2. The black lines joining the two tracks connect vehicle positions at the same point in time. The dotted blue and red lines represent the waypoint paths that vehicle 1 and vehicle 2 were attempting to follow, respectively.

Poor acoustic communications during this first run resulted in repeated leadership changes. When testing with more than two vehicles, it is possible to share knowledge of the fleet through 13-bit messages, but with only two vehicles a missed communication will cause the other vehicle to assume the leader has been lost and take on the leadership role. This constant switching of leadership caused both vehicles to maintain a steady speed since the leader does not adjust speed.

Vehicle 2 moved its own formation position halfway through the run to fill an empty formation position. The formation was started with an empty position to test this part of the control algorithm. The formation change is why the two tracks and waypoint paths are much closer during the final leg of the course than on the first leg.

Fig. 4 shows a plot of vehicle positions during a second formation run. During this run vehicle 2 aborted the mission early due to discrepancies between the on-board navigation estimate and acoustic range information. As in the first formation run, vehicle 2 was moved to fill a vacant formation position. This is why the waypoint path shifts halfway through the first leg of the course. Throughout the run vehicle 1 was the leader and kept a constant speed. Fig. 5 shows a plot of the motor RPM recorded by vehicle 2 during the run. Every 15 seconds a 32-byte message was received from vehicle 1 containing the progress of the leader. Vehicle 2 then adjusted motor RPM to maintain the correct relative distance to the leader, *d.* The vehicles must maintain a motor speed of at least 700 RPM to maintain depth.

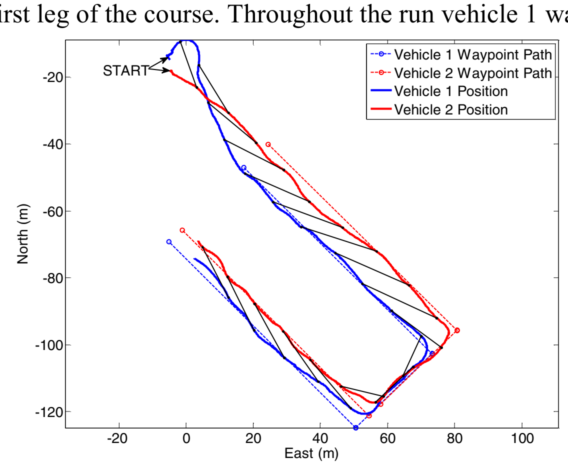

Figure 3. Plot of vehicle positions during first formation mission.

It is difficult to estimate the navigation accuracy because topside tracking points were only available every 15 seconds due to the communication cycle. The data does show that the position estimate was within 0.75 m of each topside tracking point.

B. Magnetic Measurement Results

During the formation runs presented in Fig. 3 and Fig. 4 the vehicles were continuously recording magnetic data. Using data recorded by the two vehicles while stationary in the same ambient field, the magnetometer outputs from the two vehicles were calibrated to each other in post-processing. The three magnetic components, B_x, B_y, and B_z, were converted into total magnetic field, B_T, using

$$B_T = \sqrt{B_x^2 + B_y^2 + B_z^2}. \tag{6}$$

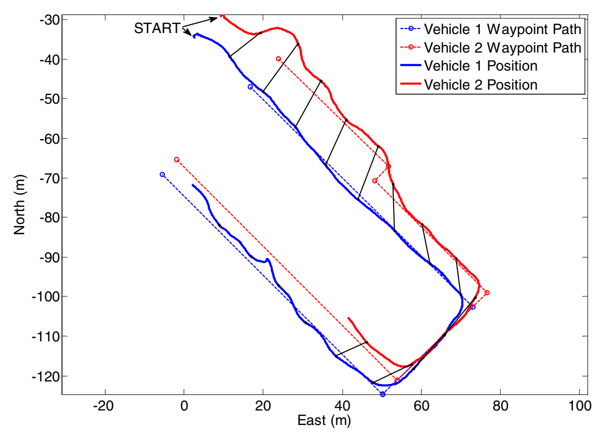

Figure 4. Plot of vehicle positions during second formation mission.

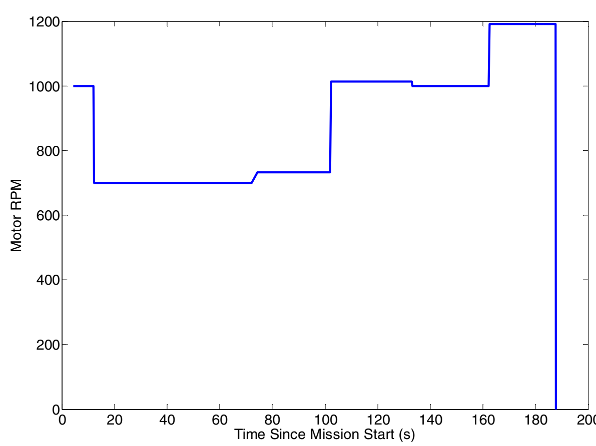

Figure 5. Motor RPM of vehicle 2 during second formation mission.

The total field measurements taken during the formation runs in Fig. 3 and Fig. 4 were combined and are presented in Fig. 6. The measurement area was broken up into square meter areas, which will be called segments. Any measurement taken by either vehicle in a segment was averaged with all other measurements taken in the same segment. There is a known offset in the data recorded by the AUVs. The ambient field in the test area was ~55,000 nT, but the vehicles reported ambient fields of ~53,000 nT. This is due to a resistor divider network loading the magnetometer outputs.

In certain areas breaks occur in the measurements such as at (E, N) = (63,-80) in Fig. 6. These breaks are introduced during post-processing of the recorded data to remove noise from acoustic modem transmissions. Recorded data is first filtered using a non-causal, seventh-order Chebyshev type 2 high pass filter with a cutoff frequency of 50 Hz. Because the acoustic transmissions cause high frequency noise in the recorded data, corrupted areas show up as peaks in the filtered data. The indexes of the peaks are noted, and then the data associated with those indexes in the original, unfiltered data are removed.

Combining the two formation runs gives enough information to see anomalies in the test area ambient field in Fig. 6. When the vehicles passed near (E, N) = (40,-40) both measured a significant decrease in total field. Vehicle 1 measured a decrease from ~53,500 nT to ~52,700 nT, and vehicle 2 measured a decrease from ~53,500 nT to ~51,500 nT. This is likely due to large steel pilings marking the border of the secured area. It is near this position that the vehicles pass closest to one of the pilings. During the final leg of the course near (E, N) = (10,-80) both vehicles again measured a decrease in the total field. Both vehicles measured an ambient field of ~53,000 nT on the final corner, and at the end of the final leg the ambient field had decreased to ~51,800 nT. During the final leg, the vehicles approached a large steel building which was likely the cause of the magnitude change.

The agreement in the measurements between vehicles and between runs is encouraging. In areas near (E, N) = (75,-95) and (E, N) = (50,-115) the tracks are within 2 m of each other but not overlapping, so the measurements from separate runs were not averaged together. The measurements from the two runs are within ~50 nT. The fact that the measurements are so close gives confidence in the measurement system.

In Fig. 7, the color of each segment represents the standard deviation of the total field data recorded in that segment. Just as with the total field plot in Fig. 6, any measurements from either vehicle in a segment were included in the standard deviation calculation. In the majority of the sampled area, the standard deviation was below 25 nT. In areas with higher standard deviations the causes were actual noise in the measurements, a small number of measurements taken in the segment, and actual ambient field gradients.

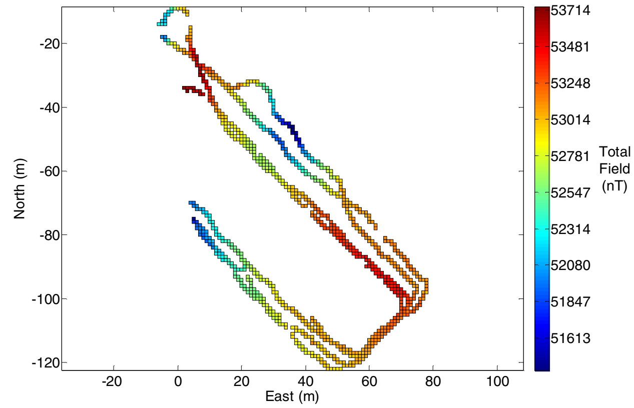

Figure 6. Average total field measured during formation runs. Color of square meter segment represents the average of all measurements taken in that square meter.

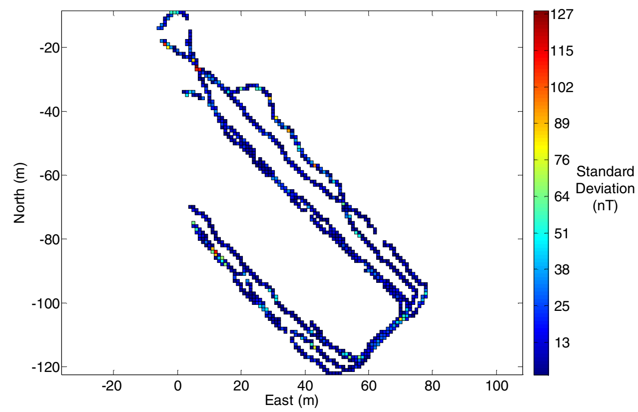

Figure 7. Standard deviation of total field measurements during formation runs. Color of square meter segment represents the standard deviation of all measurements taken in that segment.

Measurements were also taken using a large steel barge as a magnetic source within the test area. Only one AUV was used for the measurements. The total field and standard deviation over two separate runs are shown in Fig. 8 and Fig. 9, respectively. Both the barge and a nearby piling appear as field fluctuations in Fig. 8. The barge created a much larger field change, lowering the field down to ~50,000 nT and alternately raising it above 62,000 nT near (E, N)=(32,-27).

The standard deviation in Fig. 9 shows that the ambient field away from magnetic sources was very slowly changing, but rapid changes in the field near the piling and barge caused high standard deviations in the measurements. This is an artifact of the spatial averaging over square meter segments of area.

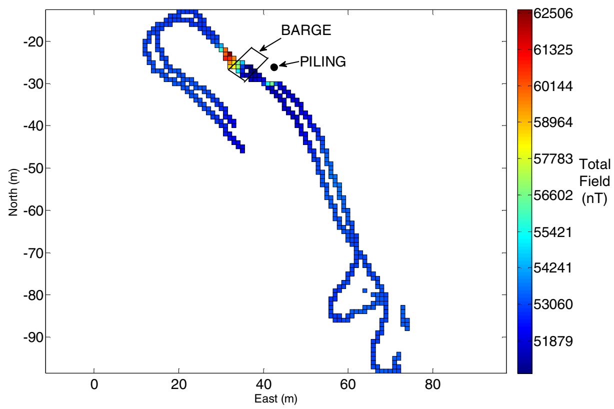

Figure 8. Average total field measured during two barge passes. Color of square meter segment represents the average of all measurements taken in that square meter.

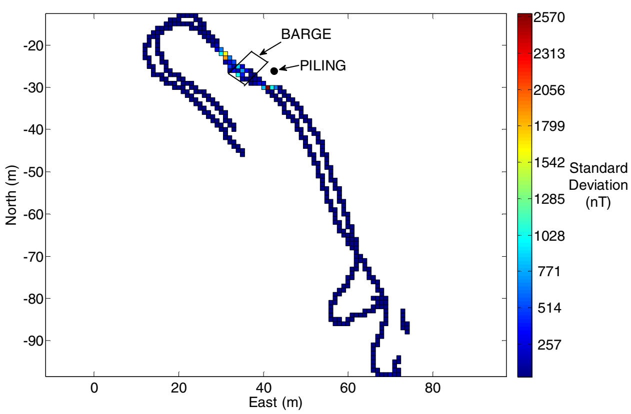

Figure 9. Standard deviation of total field measurements during two barge passes. Color of square meter segment represents the standard deviation of all measurements taken in that segment.

VI. CONCLUSIONS AND FUTURE WORK

This paper has described AUVs and a formation control algorithm utilized in initial tests with the objective of measuring ambient magnetic field. Test data shows that the formation control algorithm worked as expected. The AUVs followed the correct waypoint paths and adjusted roles to fill empty formation positions. The magnetic measurements show repeatability between runs and low amounts of noise in the measurements. Variations in the ambient magnetic field of ~1,000-2,000 nT were detected by the AUVs. Also, repeated measurements of a large steel barge showed consistent magnetic field fluctuations from ~50,000 nT up to ~62,000 nT. The measurements taken in slowly changing ambient fields had standard deviations at or below 25 nT in each segment. This indicates repeatability and low noise in the measurement system.

Continued measurements to map the magnetic field in the secured area at ARD are planned. Additional vehicles are under construction to increase the number of measurement-ready vehicles. Adding vehicles to the formation will improve formation control due to the sharing of information that occurs between vehicles. Also, additional work is being done on reducing noise in the magnetic measurements caused by the induced field of the AUV.

Due to the number of large metal structures in the secured area, a second tracking system is being installed in an open water area in Lake Pend Oreille. This second tracking range will allow for measurements of the signature of surface ships in a magnetically clean environment. Fleet measurements of the ambient field in this new range are also planned to map any unknown sources of magnetic fields.

ACKNOWLEDGMENT

The authors gratefully acknowledge the support of the Office of Naval Research, through “Electromagnetic Signature Assessment System Using Multiple Autonomous Underwater Vehicles (AUVs)”, ONR N00014-08-1-0779.

REFERENCES

[1] E. Bovio, D. Cecchi, and F. Baralli, “Autonomous underwater vehicles for scientific and naval operations”, *Annual Reviews in Control*, vol. 30, pp. 117-130, Issue 2, 2006.

[2] M. Grasmueck, G. P. Eberli, D. A. Viggiano, T. Correa, G. Rathwell, and J. Luo, “Autonomous underwater vehicle (AUV) mapping reveals coral mound distribution, morphology, and oceanography in deep water of the Straits of Florida”, *Geophys. Res. Lett,* vol. 33, 2006.

[3] K. R. Newman, M. H. Cormier, J. K. Weissel, N. W. Driscoll, M. Kastner, E. A. Solomon, G. Robertson, J. C. Hill, H. Singh, R. Camilli, and R. Eustice, “Active methane venting observed at giant pockmarks along the U.S. mid-Atlantic shelf break”, *Earth and Planetary Science Letters*, vol. 267, pp. 341-352, Issues 1-2, March 2008.

[4] E. Fiorelli, N. E. Leonard, P. Bhatta, D. Paley, R. Bachmayer, and D. Fratantoni, “Multi-AUV control and adaptive sampling in Monterey Bay”, *2004 IEEE/OES Autonomous Underwater Vehicles*, pp. 134-147, 2004.

[5] L. Freitag, M. Grund, C. von Alt, R. Stokey, and T. Austin, “A shallow water acoustic network for mine countermeasures operations with autonomous underwater vehicles”, *Underwater Defense Technology (UDT) 2005*, 2005.

[6] S. Willcox, D. Goldberg, J. Vaganay, and J. Curcio, “Multi-vehicle cooperative navigation and autonomy with the Bluefin CADRE system”, in *Proceedings of IFAC (International Federation of Automatic Control) Conference*, Lisbon, Portugal, Sept, 2006.

[7] J. Curcio, J. Leonard, J. Vaganay, A. Patrikalakis, A. Bahr, D. Battle, H. Schmidt, and M. Grund, “Experiments in moving baseline navigation using autonomous surface craft”, *OCEANS 2005 Proceedings of MTS/IEEE*, vol. 1, pp. 730-735, 2005.

[8] J. Rice, “Seaweb acoustic communication and navigation networks”, *Proceedings of the International Conference “Underwater Acoustic Networks: Technologies and Results”*, July 2005.

[9] I. Vasilescu, K. Kotay, D. Rus, M. Dunbabin, and P. Corke. “Data collection, storage, and retrieval with an underwater sensor network”. *Proceedings of the 3rd international conference on Embedded networked sensor systems,* pp 154-165, 2005.

[10] M. Dunbabin, P. Corke, I. Vasilescu, and D. Rus, “Experiments with cooperative control of underwater robots,” *International Journal of Robotics Research*, vol. 28, pp. 815 – 833, June 2009.

[11] R. Haraksim, L. Brignone, and J. Opderbecke, “Multiple AUV control in an operational context: a leader - follower approach,” in *Proc. OCEANS 2009-EUROPE, 2009. OCEANS '09*, Bremen, May 2009.

[12] L. Brignone, J. Alves, and J. Opderbecke, “GREX sea trials: first experiences in multiple underwater vehicle coordination based on acoustic communication,” in *Proc. OCEANS 2009-EUROPE, 2009. OCEANS '09*, Bremen, May 2009.

[13] J. B. Nelson and T. C. Richards, “Magnetic source parameters of MR OFFSHORE measured during trial MONGOOSE 07,” Tech. Rep., Defence R&D—Atlantic, Dartmouth NS, Canada, 2007.

[14] B. Armstrong, J. Pentzer, D. Odell, T. Bean, J. Canning, D. Pugsley, J. Frenzel Michael Anderson, and D. Edwards, “Field measurement of surface ship magnetic signature using multiple AUVs”, *Proceedings MTS/IEEE Oceans 09*, 2009.

[15] D. J. Stilwell, A. S. Gadre, C. A. Sylvester, and C.J. Cannell, , "Design elements of a small low-cost autonomous underwater vehicle for field experiments in multi-vehicle coordination," *Autonomous Underwater Vehicles, 2004 IEEE/OES* , vol., no., pp. 1- 6, June 2004

[16] L. Freitag, M. Grund, S. Singh, J. Partan, P. Koski, and K. Ball, "The WHOI micro-modem: an acoustic communications and navigation system for multiple platforms," *OCEANS, 2005. Proceedings of MTS/IEEE* , vol. 2, pp.1086-1092, Sept. 2005.

[17] J. Pentzer, B. Armstrong, D. Odell, T. Bean, J. Canning, M. Anderson, and D. Edwards, “On-the-fly measurement of surface ship acoustic and magnetic signature using multiple AUVs”, *Proceedings of MSS Battlespace Acoustic and Seismic Sensing, Magnetic & Electric Field Sensors (BAMS) Symposium*, 2009.

[18] B. Armstrong, E. Wolbrecht, D. Odell, and D. Edwards, “AUV navigation with an extended kalman filter in a magnetic disturbance,” *OCEANS’ 10 IEEE Sydney,* in press.

[19] M. S. Grewal and A. P. Andrews, (2008). *Kalman filtering: Theory and practice using MATLAB®*. Hoboken, N.J.: John Wiley & Sons.

[20] H. E. Rauch, F. Tung, and C. T. Striebel, “Maximum likelihood estimates of linear dynamic systems,” *AIAA Journal*, vol. 3, no. 8, pp. 1445-1450, Aug. 1965.

[21] T. Bean, et al., "Language and logic to enable collaborative behavior among multiple autonomous underwater vehicles," *International Journal of Intelligent Control and Systems*, vol. 13, pp. 67-80, Jan. 2008.

[22] D. B. Edwards, T. Bean, D. Odell, and M.J. Anderson, "A leader-follower algorithm for multiple AUV formations", *2004 IEEE/OES Autonomous Underwater Vehicles*, Sebasco Estates, Maine, June 2004.

[23] A. Okamoto and D.B. Edwards, “Regulating a formation of a large number of vehicles,” *Proceedings of the 2005 ASME International Mechanical Engineering Congress and Exposition, Orlando, Florida*, November, 2005.

[24] A. Okamoto, J. Feeley, D. Edwards, and R. Wall, “Robust control of a platoon of underwater autonomous vehicles,” *Oceans’04 Techno-Ocean’04 (OTO’04) Conference Proceedings*, pp. 505-510, 2004.

[25] A. Okamoto, “Robust control of a platoon of autonomous underwater vehicles”, MSEE Thesis, University of Idaho, 2003.

[26] L. Lapierre, D. Soetanto, and A. Pascoal, “Coordinated motion control of marine robots”, Proceedings 6th IFAC Conference on Manoeuvering and Control of Marine Craft (MCMC2003), Girona, Spain, 2003.

[27] R. Ghabcheloo, A. Pascoal, C. Silvestre, and I. Kaminer, “Coordinated path-following control of multiple AUVs in the presence of communication failures and delays”, *International Journal of Systems Science*, vol. 37, no. 6, pp 399-405, 2006.